Pergamon

PII: S0360-3199(96)00075-4

Int. J. Hydrogen Energy, Vol. 22, No. 1, pp. 57–62, 1997

Elsevier Science Ltd
Printed in Great Britain.
0360-3199/97 $17.00 + 0.00

PHOTOCATALYTIC HYDROGEN PRODUCTION BY DYE-SENSITIZED Pt/SnO_2 AND $Pt/SnO_2/RuO_2$ IN AQUEOUS METHYL VIOLOGEN SOLUTION

K. GURUNATHAN, P. MARUTHAMUTHU* and M. V. C. SASTRI

Department of Energy, University of Madras, Guindy Campus, Madras 600 025, India

(*Received* 12 *April* 1996)

Abstract—Hydrogen photoproduction by a rarely studied, wide band gap semiconductor, SnO_2, in powder form loaded with Pt and RuO_2 and sensitized by $Ru(bpy)_3^{2+}$ and organic dyes or with low band gap semiconductor, CdS, was investigated. Acriflavin, Eosin Blue, Rhodamine B, Rose Bengal and Fluorescein were used as photosensitizers in the presence of methyl viologen and with or without a sacrificial agent, EDTA. The effects of variation in concentrations of $Ru(bpy)_3^{2+}$ and MV^{2+} were studied. The maximum rate of hydrogen production was observed at $[Ru(bpy)_3^{2+}] = 3.75 \times 10^{-5}$ mol dm^{-3} and $[MV^{2+}] = 2.5 \times 10^{-5}$ mol dm^{-3}. The efficiency of the sensitizers in hydrogen production was found to decrease in the order: Eosin Blue > Rose Bengal > $Ru(bpy)_3^{2+}$ > rhodamine B = acriflavin > fluorescein. Copyright © 1996 International Association for Hydrogen Energy

INTRODUCTION

The splitting of water into hydrogen and oxygen by visible light is of great importance in the context of development of alternative fuel sources. Photocatalytic and photoelectrochemical processes offer a promising method for this purpose [1–4]. Chalcogenide semiconductors are used as photocatalysts for the water splitting reaction but they are prone to undergo photocorrosion. To avoid this, oxide semiconductors are used. Unfortunately, most of the oxides have wide band gaps and absorb little visible light. Hence, doping or external sensitization of the wide band-gap semiconductors is adapted to perform effective photocatalytic reactions in visible light.

SnO_2 exhibits a good activity and stability during irradiation, both in acidic and basic media [5]. However, the disadvantage of this material is its wide band gap ($E_g = 3.5$ eV), which necessitates the use of near UV light band-gap excitation. The photochemical properties of wide band gap semiconductor particles can be altered physically or chemically by modifying their environment. In order to extend the light absorption of SnO_2 in the visible region, it may be possible to sensitize it externally by organic photosensitizers or low band gap semiconductors like CdS. In photocatalytic hydrogen production using methyl viologen as the electron relay ($E^0 = -0.44$ V), synthetic dyes are chosen as photosensitizers which have reduction potentials more negative than -0.44 V to sensitize wide band gap semiconductors [6]. In the presence of semiconductors, the dye sensitization involves the interaction of the dye with the semiconductors facilitating charge injection into the conduction band of the semiconductor.

Electron transfer reactions with colloidal SnO_2 have been examined by the use of radiolytically generated reducing radicals, direct band gap excitation and photosensitization by $Ru(bpy)_3^{2+}$ [7]. Memming and Schropel [8] have shown that the luminescence of long chain derivatives of $Ru(bpy)_3^{2+}$ is quenched by an electron transfer reaction at the surface of SnO_2 electrode. It has also been found that the luminescence from $*Ru(bpy)_3^{2+}$ adsorbed on SnO_2 powder, is quenched by an electron transfer process from excited $Ru(bpy)_3^{2+}$ to the semiconductor [9]. Steady state illumination of an aqueous solution of $Ru(bpy)_3^{2+}$ in the presence of a suitable electron donor may, therefore, be expected to build up electrons on colloidal SnO_2. Mulvaney *et al.* [7] have studied the photochemical generation of MV^{+} by excitation of SnO_2 colloid.

The electrochemical behaviour of SnO_2 electrodes [10, 11] reveals that oxygen evolution proceeds via the valence band whereas most reduction processes occur via the conduction band of SnO_2. Photoeffects at polycrystalline SnO_2 electrodes have been demonstrated by Kim and Latinen [12]. The photoassisted electrolysis of water by UV radiation of a Sb/SnO_2 electrode has been studied by Wrighton *et al.* [13].

In the present investigation, an attempt is made for the photocatalytic production of hydrogen with SnO_2 semiconductor particulates loaded with Pt/RuO_2 and

CdS. The effects of variation of $[Ru(bpy)_3^{2+}]$, $[MV^{2+}]$ and the use of various organic dyes on the photocatalytic hydrogen production have been presented.

EXPERIMENTAL

Materials

Purest research grade SnO_2 (99.99%) and methyl viologen were from Aldrich, U.S.A. and were used as such. H_2PtCl_6, RuO_2 and $RuCl_3 \cdot 3H_2O$ were from Johnson Mathey Chemicals, U.K. Other chemicals used were of analytical reagent grade.

Preparation of photocatalysts

$Ru(bpy)_3Cl_2$ was prepared by refluxing 2,2′-bipyridyl (2.0 g, 25% excess) and $RuCl_3 \cdot 3H_2O$ in 95% ethanol for 72 h [14]. SnO_2, H_2PtCl_6 ([Pt] = 0.5 w/w%) and RuO_2 (0.5 w/w%) were mixed in water, stirred for 1 h and dried at 100°C. The powder was crushed and sintered in the temperature range 800–1000°C in a tubular furnace for 16 h in an argon atmosphere. It was then ground to fine powder and used as the photocatalyst. Similarly, CdS powder (10 w/w%) was mixed with SnO_2 powder and sintered at 500°C in argon atmosphere for 3 h.

Characterization of photocatalysts

The diffuse absorption spectra of the undoped and doped SnO_2 powders were recorded by a Varian Spectrophotometer (Model Cary 2300) equipped with an integrating sphere. The base line correction was done using a calibrated sample of $BaSO_4$ from wavelength 250 to 800 nm. The difference absorption spectra of doped SnO_2 powders were obtained by plotting the difference in absorption between the two spectra (doped and undoped) at different wavelengths. The crystal structures were determined by the X-ray diffraction method (Phillips X-ray Diffractometer, PW 1130; radiation = CuK_α, $\lambda = 1.5418$ Å). The particle size was 1–5 μm and the surface areas of the samples, estimated by Quantasorb surface area measurement, were 10–13 $m^2\ g^{-1}$.

Procedure for hydrogen production

Typically, 80 mg of the photocatalyst powders were dispersed in 80 ml of methylviologen solution ($[MV^{2+}] = 1 \times 10^{-5}$ mol dm^{-3}) at 25°C, deaerated with argon for 1 h and illuminated with light from a 150 W xenon arc lamp. IR radiation was cut-off by using water jacket prior to irradiation of the sample. The light intensity of the lamp was determined by potassium ferrioxalate actinometry [15] ($I_o = 0.5 \times 10^{-8}$ Eins $s^{-1}\ cm^{-2}$). During the photocatalytic experiments, the evolved gas was passed through alkaline pyrogallol solution at 0–5°C to remove oxygen (if formed due to water oxidation by h^+_{VB}) and the rest of the gas was collected in a water manometer. The collected gas was identified as hydrogen by GC (Chromatography and Instruments Company, India) using a Porapak Q column and argon as the carrier gas.

Estimation of quantum yield

The quantum yields for photocatalytic hydrogen production for undoped/doped SnO_2 were calculated using the formula,

$$\phi = \frac{\text{number of hydrogen atoms formed per s}}{\text{number of photons absorbed per s}}. \quad (1)$$

The denominator in equation (1), is derived from the diffuse absorption spectral studies. The diffuse absorption spectra of different doped samples show that they do not absorb 100% incident radiation at 350 nm but a fraction of the total incident radiation and the amount of absorption differs for different samples (Fig. 1A and B). Therefore, the actual number of Einsteins absorbed, I_a, by a sample per unit time, was calculated as,

Number of Einsteins absorbed per s by a sample =

$$\frac{I_0 \times \%\ \text{absorption of the sample at } \lambda = 350\,\text{nm}}{100}, \quad (2)$$

where I_0 = intensity of the incident light.

Hence,

quantum yield (ϕ) =

$$\frac{2 \times \text{hydrogen gas evolution rate (M s}^{-1})}{\text{rate of photon absorption (Einstein s}^{-1})}. \quad (3)$$

RESULTS AND DISCUSSION

Figure 1(A) shows the diffuse absorption spectra of (a) undoped SnO_2 (b) 1 at% Pt/SnO_2 and (c) 10 w/w% CdS/SnO_2 photocatalysts and Fig. 1(B) shows the difference absorption spectra of (a) and (b), and (a) and (c). Pt loading is found to enhance the visible light absorption of SnO_2, and CdS loading extends the light absorption with a peak at 500 nm. The X-ray diffractograms of the processed SnO_2, 1 at% Pt/SnO_2 and 10 w/w% CdS/SnO_2 photocatalysts show the presence of new peaks. The new peaks due to CdS are distinctly visible. Hence, there is an increase in the crystallinity in Pt/SnO_2 and CdS/SnO_2 compared to SnO_2. The peak heights of the lines due to Pt/SnO_2 and CdS/SnO_2 are found to be decreased compared to those due to the processed SnO_2.

Photocatalytic hydrogen production by undoped/doped SnO_2 in the presence of MV^{2+} and EDTA

Table 1 presents the amounts of hydrogen produced and their quantum yields in the presence and absence of photosensitizer, MV^{2+} and sacrificial agent, EDTA. A maximum yield of hydrogen is observed with the $Pt/SnO_2/RuO_2$–$Ru(bpy)_3^{2+}$–MV^{2+}–EDTA system due to (1) the loading of bifunctional redox catalyst on SnO_2, (2) electron injection from excited $Ru(bpy)_3^{2+}$ to conduc-

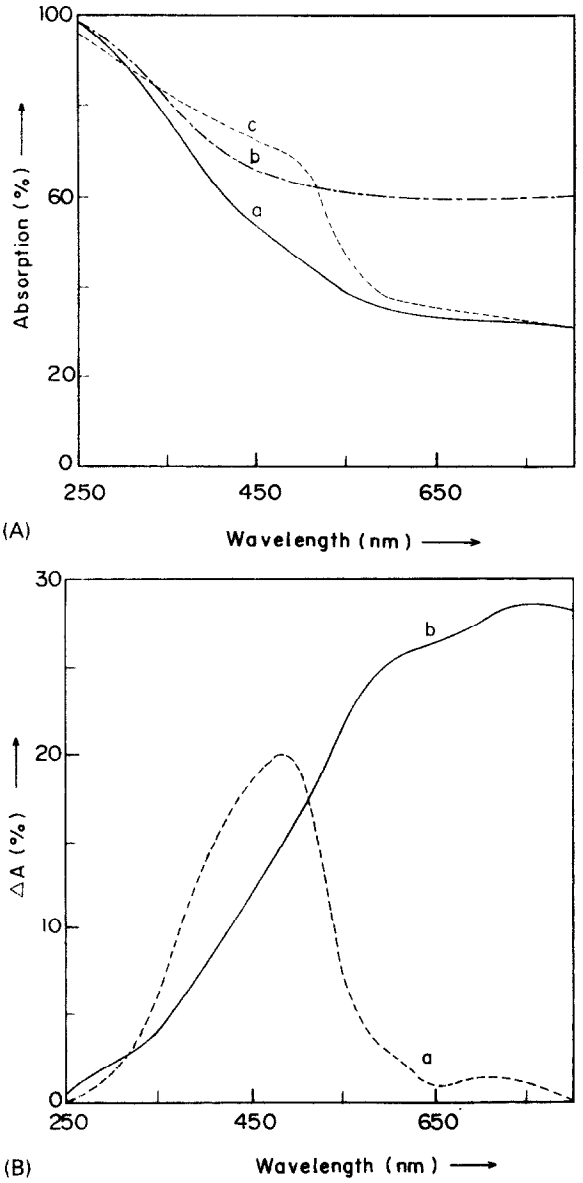

Fig. 1. (A) Diffuse absorption spectra of (a) processed SnO_2; (b) 1.0 atomic% Pt/SnO_2; (c) 10.0 w/w% CdS/SnO_2. (B) Difference absorption spectra of (a) 10.0 w/w% CdS/SnO_2; (b) 1.0 atomic% Pt/SnO_2.

tion band of SnO_2, (3) electron mediation by MV^{2+} and (4) electron donation by the EDTA to scavenge the valence band holes. Table 2 shows that the increase in the concentrations of $Ru(bpy)_3^{2+}$ up to 3.75×10^{-5} mol dm^{-3} enhances the hydrogen production rate, after which it reaches a saturation limit at 5.0×10^{-5} mol dm^{-3}. This is due to the fact that with increasing $[Ru(bpy)_3^{2+}]$, the potential of the catalyst particles becomes more negative and the mass transfer of $MV^{\cdot+}$ to the surface of the catalyst becomes a less important rate determining factor. The increase in $[Ru(bpy)_3^{2+}]$ may increase the formation of $MV^{\cdot+}$ in solution. However, the influence of the sensitizer concentration beyond this limit diminishes, because most of the light appropriate for excitation is already absorbed at this level of concentration. Any further increase of the $[Ru(bpy)_3^{2+}]$ does not significantly affect the excitation (S*) rate. A decrease in the hydrogen production rate above 5×10^{-5} mol dm^{-3} of $Ru(bpy)_3^{2+}$ has been attributed to an inner filter effect [16].

$[MV^{2+}]$ *variation*

Table 3 presents the effect of MV^{2+} concentration on photocatalytic hydrogen production with Pt/SnO_2 photocatalyst. An increase in the concentration of MV^{2+} at 1.25 and 2.5×10^{-5} mol dm^{-3} increases the hydrogen production and beyond 5×10^{-5} mol dm^{-3}, the rate decreases. At higher concentrations of MV^{2+}, the $MV^{\cdot+}$ formed may dimerize. The reduction potential of the dimer is lower than that of the monomer, thereby making the evolution of hydrogen thermodynamically less favourable [17]. Moreover, the bulk concentration of $MV^{\cdot+}$ would indeed increase leading to the ultimate result of a decline in the rate of hydrogen production and combination of these two effects causes the retardation in rate. Also, at higher concentrations, MV^{2+} slows down the heterogeneous reaction by adsorption on the catalyst surface, thereby blocking the reaction sites [18].

Pt/SnO_2–MV^{2+}–*various sensitizers*

Figure 2 presents the photocatalytic hydrogen production by Pt/SnO_2 sensitized with various photosensitizers, $Ru(bpy)_3^{2+}$, acriflavin, Eosin Blue, rhodamine B, Rose Bengal and fluorescein. Of all the photosensitizers used, Eosin Blue shows a maximum efficiency to sensitize SnO_2 and evolves a greater amount of hydrogen. The efficiency of the sensitizers for the photocatalytic hydrogen production in this system is found to be in the decreasing order, Eosin Blue > Rose Bengal > $Ru(bpy)_3^{2+}$ > rhodamine B = acriflavin > fluorescein. Each sensitizer has its own characteristic efficiency and there is no correlation between this and its properties [6] namely, redox potentials and λ_{max} of absorption given in Table 4 or its structure. Hence, a general conclusion cannot be drawn from the above order based on either the structure or the properties of the sensitizers.

Photocatalytic hydrogen production using 10 w/w% CdS/SnO_2–MV^{2+}–*EDTA*

An important approach to prevent the quick e^-–h^+ recombination in photocatalysis is the coupling of semiconductor particles with different energy levels [19, 20]. In the CdS–SnO_2 system, photogenerated electron from CdS (E_g = 2.4 eV) can be transferred into a SnO_2 particle while the holes remain in the CdS particle. The scheme explaining the valence and conduction bands of the CdS–SnO_2 is shown in Scheme 1. This process of charge separation is considered to be very fast, for example, a picosecond laser flash photolysis study of CdS–TiO_2 has

Table 1. Amounts and quantum yields of photocatalytic hydrogen production by Pt and RuO_2 loaded SnO_2

$[MV^{2+}] = 1.25 \times 10^{-5}$ mol dm^{-3}
$[Ru(bpy)_3^{2+}] = 2.50 \times 10^{-5}$ mol dm^{-3}
[Pt] = 0.5 w/w%
[RuO_2] = 0.5 w/w%
[EDTA] = 2×10^{-2} mol dm^{-3}
T = 298 K
pH 7

System	Vol. of H_2 evolved (ml h^{-1})	Turnover number	Amount of H_2 evolved (μM h^{-1})	Quantum yield
SnO_2	—	—	—	—
$SnO_2 + MV^{2+}$	—	—	—	—
$S + MV^{2+}$	—	—	—	—
$S + MV^{2+} + EDTA$	—	—	—	—
$SnO_2 + MV^{2+} + S$	0.06	0.16	2.68	0.11
$Pt/SnO_2 + MV^{2+}$	0.26	0.70	11.60	0.52
$Pt/SnO_2 + MV^{2+} + S$	0.46	1.24	20.52	0.89
$Pt/SnO_2/RuO_2$	—	—	—	—
$Pt/SnO_2/RuO_2 + MV^{2+}$	0.79	2.12	35.23	1.54
$Pt/SnO_2/RuO_2 + MV^{2+} + S$	1.12	3.01	49.95	2.18
$Pt/SnO_2 + MV^{2+} + S + EDTA$	1.13	3.03	50.40	2.20
$Pt/SnO_2/RuO_2 + MV^{2+} + S + EDTA$	1.23	3.30	54.85	2.40
$S + MV^{2+} + Pt + EDTA$	0.30	0.81	13.38	—
$S + MV^{2+} + Pt + RuO_2 + EDTA$	0.46	1.24	20.52	—
$S + MV^{2+} + RuO_2 + EDTA$	0.39	1.04	17.39	—

S = Photosensitizer = $Ru(bpy)_3^{2+}$.

Table 2. Effect of $[Ru(bpy)_3^{2+}]$ on photocatalytic hydrogen production using 1 at% Pt/SnO_2 ($[MV^{2+}] = 1.25 \times 10^{-5}$ mol dm^{-3}; T = 298 K)

$[Ru(bpy)_3^{2+}] \times 10^5$ (mol dm^{-3})	Amount of H_2 evolved (μM h^{-1})	$2 \times H_2$ rate (mol dm^{-3})	Quantum yield
0.00	11.60	0.64	0.50
1.25	11.60	0.64	0.50
2.50	14.72	0.82	0.65
3.75	37.91	2.10	1.65
5.00	37.91	2.10	1.65
6.25	17.39	0.96	0.75
10.00	11.60	0.64	0.50

Table 3. Effect of $[MV^{2+}]$ on photocatalytic hydrogen production using 1 at% Pt/SnO_2 ([Rose Bengal] = $2.5 \times$ mol dm^{-3}; T = 298 K)

$[MV^{2+}] \times 10^5$ (mol dm^{-3})	Amount of H_2 evolved (μM h^{-1})	$2 \times H_2$ rate (mol dm^{-3})	Quantum yield
0.00	14.72	0.82	0.64
1.25	41.03	2.26	1.78
2.50	49.95	2.78	2.19
5.00	49.95	2.78	2.19
7.50	32.11	1.78	1.40
10.00	29.44	1.64	1.29

shown that the electron injection from CdS into TiO_2 occurs in less than 20 ps [18]. Figure 3 presents the amount of hydrogen produced with 10 w/w% CdS/SnO_2 photocatalyst in the presence of methylviologen and with or without EDTA. A sacrificial electron donor, EDTA in this system is employed to scavenge the holes formed on illumination which otherwise would decompose the CdS semiconductor. From Fig. 3, it is understood that

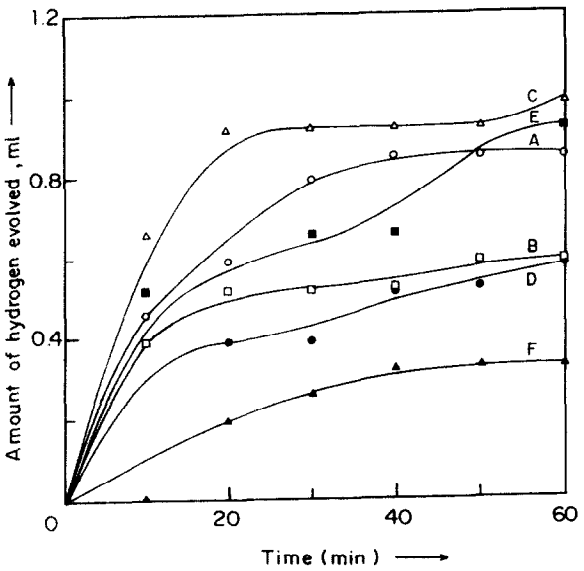

Fig. 2. Photocatalytic hydrogen production by Pt/SnO_2 sensitized by various sensitizers. (A) $Ru(bpy)_3^{2+}$; (B) acriflavin; (c) Eosin Blue; (D) rhodamine B; (E) Rose Bengal and (F) fluorescein.

in the presence of EDTA, the catalyst evolves greater amounts of hydrogen than in the absence of EDTA. The probable reactions are:

$$CdS \xrightarrow[\lambda \geq 500\,nm]{h\nu} e^-_{CB}(CdS) + h^+_{VB} \quad (4)$$

$$e^-_{CB}(CdS) + SnO_2 \rightarrow e^-_{CB}(SnO_2) + CdS \quad (5)$$

$$2\,h^+_{VB} + EDTA \rightarrow EDTA_{ox} \quad (6)$$

$$e^-_{CB}(CdS) + H_2O \rightarrow \tfrac{1}{2}H_2 + OH^- \quad (7)$$

$$e^-_{CB}(SnO_2) + MV^{2+} \rightarrow MV^{\cdot+} + SnO_2 \quad (8)$$

$$MV^{\cdot+} + H^+ \rightarrow \tfrac{1}{2}H_2 + MV^{2+}. \quad (9)$$

Light is absorbed by the CdS particles producing $e^- - h^+$ pairs (equation 4). The holes are scavenged by EDTA generating oxidized products of EDTA (equation 6). The complimentary reactions of e^-_{CB}, competing with $e^- - h^+$ recombination are reduction of water to hydrogen and

Table 4. One-electron reduction potential and λ_{max} of absorption of the photosensitizers used for sensitization of SnO_2

Sensitizer	One-electron reduction potential, V vs NHE	λ_{max} (nm)
$Ru(bpy)_3^{2+}$	−0.860	452
Acriflavin	−0.650	454
Eosin Blue	−0.580	515–518
Rhodamine B	−0.545	551–553
Rose Bengal	−0.533	544–548
Fluorescein	−0.577	491

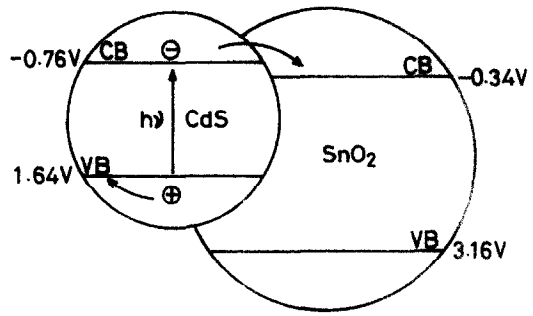

Scheme 1. Charge transfer processes in a CdS–SnO_2 coupled semiconductor system.

the interparticle electron transfer from CdS to SnO_2. The difference in energy levels of the CdS and SnO_2 semiconductors play an important role. The trapped conduction band electron by SnO_2 generate hydrogen via $MV^{2+}/MV^{\cdot+}$.

A comparison of the results of the present investigation with those of the similar work on photoreduction of methylviologen sensitized by various metal ions incorporated chlorophyll for hydrogen evolution in visible light reported by Koiso *et al.* [21], reveals a higher efficiency of hydrogen production in the present investigation. Koiso *et al.* have observed a maximum efficiency of 0.4 with Znchla, whereas Pt/SnO_2/Eosin Blue/MV^{2+} exhibits a maximum efficiency in the present investigation.

CONCLUSION

Even though SnO_2 is a wide band gap semiconductor, an attempt is made to improve its photocatalytic efficiency when it is sensitized with dyes or coupled with

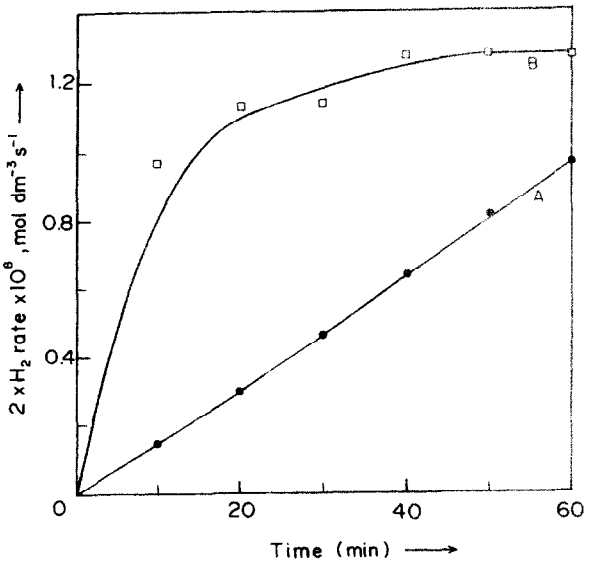

Fig. 3. Hydrogen production by 10 w/w% CdS/SnO_2 with or without EDTA. (A) Without EDTA and (B) with EDTA.

CdS. CdS loading on SnO_2 enhances hydrogen production efficiency of SnO_2 powder. Of all the organic dyes, Eosin Blue is the best sensitizer for sensitizing SnO_2. The maximum rate of hydrogen production (Tables 2 and 3) was achieved by using Pt/SnO_2 in the presence of $[Ru(bpy)_3^{2+}] = 3.75 \times 10^{-5}$ mol dm^{-3} and $[MV^{2+}] = 2.5 \times 10^{-5}$ mol dm^{-3}.

REFERENCES

1. J. S. Connolly (ed.) Photochemical Conversion and Storage of Solar Energy (Proc. III International Conference). Academic Press, New York (1981).
2. J. Sabata, S. C. March, R. Simoro and J. Gimenez, *Int. J. Hydrogen Energy* **15**, 115 (1990).
3. A. Fujishima and K. Honda, *Bull. Chem. Soc. Jpn* **44**, 1148 (1971).
4. A. B. Ellis, S. W. Kaiser, and M. S. Wrighton, *J. Phys. Chem.* **80**, 1325 (1976).
5. D. E. Scaife, *Solar Energy* **25**, 41 (1980).
6. M. S. Chan and J. R. Bolton, *Solar Energy* **24**, 561 (1980).
7. P. Mulvaney, F. Grieser and D. Meisel, *Langmuir* **6**, 567 (1991).
8. R. Memming and F. Schropel, *Chem. Phys. Lett.* **62**, 207 (1979).
9. K. Hashimoto, M. Hiramoto, A. B. P. Lever and T. Sakata, *J. Phys. Chem.* **92**, 1016 (1988).
10. N. Armstrong, A. Lin, M. Fujihira and T. Kuwana, *Anal. Chem.* **48**, 741 (1976).
11. H. Latinen, C. Vincent and T. Bednarski, *J. Electrochem. Soc.* **115**, 1024 (1968).
12. H. Kim and H. A. Latinen, *J. Electrochem. Soc.* **122**, 53 (1975).
13. M. S. Wrighton, D. L. Morse, H. B. Ellis, D. S. Ginley and H. B. Abrahamson, *J. Am. Chem. Soc.* **98**, 44 (1976).
14. R. A. Palmer and T. S. Piper, *Inorg. Chem.* **5**, 864 (1966).
15. C. G. Hatchard and C. A. Parker, *Proc. Roy. Soc.* **A235**, 518 (1956).
16. J. M. Kleijn, E. Rouwendal, H. P. Van Leeuwen and J. Lyklema, *J. Photochem. Photobiol. A: Chem.* **44**, 29 (1988).
17. E. M. Kosower and J. L. Cotter, *J. Am. Chem. Soc.* **86**, 5524 (1964).
18. O. Enea, *Electrochim. Acta* **30**, 13 (1985).
19. K. R. Gopidas, M. Bohorquez and P. V. Kamat, *J. Phys. Chem.* **94**, 6435 (1990).
20. B. Patrick and P. V. Kamat, *J. Phys. Chem.* **96**, 1423 (1992).
21. T. Koiso, M. Okuyama, T. Sakata and T. Kawai, *Bull. Chem. Soc. Jpn* **55**, 2659 (1982).